ELSEVIER

Field Crops Research 72 (2001) 67–91

Field Crops Research

www.elsevier.com/locate/fcr

Simulating growth, development, and yield of tillering pearl millet II. Simulation of canopy development

E.J. van Oosterom[a,*], P.S. Carberry[b], J.N.G. Hargreaves[b], G.J. O'Leary[a,1]

[a]*International Crops Research Institute for the Semi-Arid Tropics, Patancheru 502 324, Andhra Pradesh, India*
[b]*CSIRO Sustainable Ecosystems/Agricultural Production Systems Research Unit, 102 Tor Street, Toowoomba, Qld 4350, Australia*

Accepted 11 May 2001

Abstract

Tillering is an important adaptive feature of pearl millet (*Pennisetum americanum* L.) to the unpredictable growing conditions of dry areas of the semi-arid tropics. Yet, this feature has largely been ignored in the development of simulation models for pearl millet. The objective of this paper is to parameterise and validate a leaf area module for pearl millet, which dynamically simulates crop leaf area from the leaf area of individual axes through simulating inter-axis competition for light. To derive parameters for the model, four cultivars (contrasting in phenology and tillering habit) were grown under well-watered and well-fertilised conditions across a range of plant densities in three experiments at two locations in India. For selected plants, observations on the number of primary basal tillers and on the number of visible, fully expanded, and senesced leaves on each axis were made twice a week throughout the growing season. Occurrence of panicle initiation (PI) was observed in two experiments only, but data were complemented by published and unpublished data, obtained for comparable cultivars. Parameters were obtained for the time from emergence to PI as a function of daylength, the leaf initiation rate, the rate of leaf and tiller appearance and the leaf senescence rate; parameters for leaf size were determined in a previous paper. Our parameter estimates compared well with published data and were, with the exception of time to PI and leaf size, mostly independent of cultivar, axis and density. Genotypic effects on productive tiller number could be attributed to differences in main shoot leaf size. Validation of the leaf area module showed that the module adequately reproduced the effects of density, photoperiod and genotype on the leaf area of individual axes and on productive tiller number. This was despite the fact that the reduction in leaf area of non-productive tillers was achieved in the module through a reduction in leaf size, whereas the crop reduced leaf area through a reduction in leaf number. Our results indicate that LAI of a tillering crop can be simulated adequately by simulating LAI from individual leaf area and incorporating the effects of competition for light.

Keywords: Leaf area; Model development; Phenology; Competition

1. Introduction

This is the second paper in a series that aims at developing a simulation model for pearl millet. The first paper (van Oosterom et al., 2001) derived parameters to estimate the potential leaf area per axis from the total number of leaves (TLN), based on bell-shaped functions that describe the area of individual

* Corresponding author. Present address: CSIRO Sustainable Ecosystems/Agricultural Production Systems Research Unit, Long Pocket Laboratories, 120 Meiers Road, Indooroopilly, Qld 4068, Australia. Tel.: +61-7-32142359; fax: +61-7-32142308.
E-mail address: erik.van.oosterom@tag.csiro.au (E.J. van Oosterom).
[1] Present address: Mallee Research Station, CSIRO Land and Water, Mallee Research Station, Private Bag 1, Walpeup, Vic. 3507, Australia.

0378-4290/01/$ – see front matter
PII: S0378-4290(01)00165-4

leaves as a function of the ordinal position of these leaves on an axis. This paper incorporates this concept into a leaf area module that simulates the green leaf area index (GLAI) of a pearl millet crop from the GLAI of individual axes, assuming that these axes compete among themselves like crops in an intercrop.

Green leaf area is an important determinant of grain and stover yield. Accurate simulation of GLAI is hence a pre-requisite for a good simulation of grain yield and biomass. Most crop growth simulation models simulate GLAI on a whole plant basis, pooling main shoots and tillers together, e.g. APSIM-nwheat (Asseng et al., 1998), CropSyst, an object oriented agricultural systems simulator (van Evert and Campbell, 1994) and the wheat models developed by O'Leary and Connor (1996) and van Keulen and Seligman (1987). Tiller number, however, is affected by both cultivar and environment, and a significant cultivar × environment interaction for fertile tiller number per plant has been reported for pearl millet by Bidinger and Raju (2000). This was a result of high- and low-tillering cultivars employing different mechanisms of adjustment to changes in resource availability, with high-tillering cultivars predominantly adjusting through a change in productive tiller number, but low-tillering ones through a change in grain yield per panicle. Results of Craufurd and Bidinger (1988b) indeed suggested that the maximum GLAI of a high-tillering cultivar was more responsive to increased assimilate availability (through daylength extension) than that of a low-tillering cultivar. An approach to model GLAI of a crop through modelling potential GLAI of individual tillers, from which actual GLAI is calculated by considering the effects of competition for resources between tillers, should have the flexibility to deal with these observed genotypic and environmental effects on GLAI, and would be particularly useful for a profusely tillering crop like pearl millet.

The first step in such an approach to model GLAI is the simulation of potential crop GLAI, defined as the maximum GLAI that can be achieved by an axis of a particular cultivar under a certain daylength, when leaf area development is not limited by resource availability. At the level of individual axes, potential GLAI has been simulated using both logistic functions representing cumulative leaf area (Carberry et al., 1993a; Meinke et al., 1998) and bell-shaped functions representing individual leaf area (Carberry et al., 1993b; Keating and Wafula, 1992). Both methods performed similarly in a comparative study for sorghum (Carberry et al., 1993a). However, given the differences between axes in leaf area profiles (van Oosterom et al., 2001), the individual leaf approach may have more flexibility to simulate genotypic differences in tiller number in response to changes in environmental conditions (Bidinger and Raju, 2000).

Adoption of an individual leaf approach to simulate leaf area involves several steps (Carberry et al., 1993a). First, the final leaf number on each axis needs to be determined. As pearl millet is a quantitative short-day plant, longer photoperiods extend the duration of the vegetative phase, resulting in higher leaf numbers per axis (Huda et al., 1984; Alagarswamy and Bidinger, 1985; Carberry and Campbell, 1985; Craufurd and Bidinger, 1989). A quantitative analysis to determine the relationship between photoperiod, duration of the vegetative phase and leaf number has not yet been performed for pearl millet. The second step is an estimate of the appearance rate of successive leaves and tillers. Both these rates have already been quantified for pearl millet (Carberry and Campbell, 1985; Craufurd and Bidinger, 1988a), but this work was largely based on a single cultivar. Genotypic differences in leaf appearance rates have been reported for sorghum (Borrell et al., 2000) and barley (van Oosterom and Acevedo, 1992). The observed rates of leaf and tiller appearance for pearl millet thus need to be verified across a wider range of cultivars. The third step is to estimate the mature lamina leaf area of individual leaves. Parameters to describe individual leaf size as a function of total leaf number, cultivar and axis have already been derived in the accompanying paper (van Oosterom et al., 2001). The next step is an estimation of the number of senesced leaves for each axis throughout the season. In sorghum, senesced leaf number is a linear function of thermal time, although the rate at which successive leaves senesce is higher before the flag leaf stage than thereafter (Borrell et al., 2000). For pearl millet, however, no such data are available. The potential green leaf area per axis can be calculated from the above parameters by subtracting the area of the senesced leaves from the area of all the leaves that have emerged.

Once potential GLAI has been determined, actual GLAI needs to be calculated. Actual GLAI will be less

than the potential if there is insufficient carbon available to sustain the potential increase in GLAI. This is the case when competition for light is intense, causing a reduction in intercepted light and hence in biomass produced. Data from a previous paper (van Oosterom et al., 2001) indicate that the size of leaves that appear during stem elongation is reduced at high plant densities as compared with low densities, both for main shoots and tillers. This competition for resources between axes is not much different from that between components of an intercrop. The main difference is that the components of an intercrop compete for resources from emergence onwards, whereas in a tillering crop, the tillers become independent of the main shoot only after they have reached a certain size. Using the analogy of an intercrop could thus be an elegant method to deal with the observed cultivar × environment interaction for tillering (Bidinger and Raju, 2000). The Agricultural Production Systems sIMulator (APSIM) (McCown et al., 1996) provides a modelling platform that has been designed to make simulation of an intercrop relatively easy, as the soil is the central module of the system. Crops can be plugged into this in parallel to simulate intercrops and APSIM has been used successfully to simulate intercrops using only parameters pertinent to the individual crops (Carberry et al., 1996). The APSIM framework thus provides an appropriate platform to simulate GLAI of a tillering crop like pearl millet based upon the simulation of competition for resources between the individual axes of a plant.

The aims of this paper were two-fold. Firstly, we derived the parameters necessary to develop a leaf area module for pearl millet, capable of simulating crop GLAI from the GLAI of individual axes. The second objective was to validate this leaf area module against field data by incorporating them into APSIM-millet.

2. Materials and methods

2.1. Cultivars

The experiments included four cultivars which were selected to represent contrasting plant types and phenology. Two of them, BJ 104 (single-cross hybrid MS 5141A × J 104) and WRajPop (a population derived from a landrace from the arid zones of northwest India), are medium early in flowering and have many productive tillers. The third cultivar, HHB 67 (single-cross hybrid 843A × H 77/833-2), also produces many tillers, but is early flowering. The fourth cultivar, RCB-IC 911 (open-pollinated variety based on germplasm from Togo), has a similar phenology to BJ 104 and WRajPop, but produces fewer albeit bigger panicles than the other genotypes. This is associated with a large leaf size and thick stems.

2.2. Experimental details

The main experiments were conducted at Patancheru, India (17°45′N, 78°16′E) during the dry season (sowing 29 February) and rainy season (sowing 26 June) of 1996. The crop was thinned to the desired plant density at about 10 days after sowing. Both experiments contained four plant densities (4, 11, 15, 20 plants m^{-2}) and were laid out as a split-plot design with three replications using plant density as the main plot. In the dry season, HHB 67 was not part of the experiment, but was used as a border. Both experiments were conducted on an alfisol (clayey-skeletal mixed isohyperthermic Udic Rhodustalf) and did not suffer from obvious drought or nitrogen stress. Details regarding crop management are given by van Oosterom et al. (2001). Additional data were collected from an experiment conducted at Jodhpur, India (26°30′N, 73°02′E). The experiment was sown on 1 July 1996 in rows 60 cm apart, and was thinned to 9 plants m^{-2} at about 10 days after sowing. It contained three N-treatments (0, 20, 40 kg N ha^{-1} supplied) and two cultivars; data on only one of them (WRajPop) will be examined here. Details on crop management have been described by van Oosterom et al. (2001). The crop received 335 mm of rain during the period 5 days prior to sowing until anthesis and a simple water budget (Frère and Popov, 1979) suggested there was little drought stress before anthesis.

Directly after thinning, at around 10 days after emergence, three representative, well-bordered plants were selected in each plot in two out of the three replications at Patancheru. At Jodhpur, five plants per N-treatment were selected from one replication. For HHB 67 in the dry season, three plants were selected from two border plots, adjacent to the experiment, for

each of two densities (4 and 15 plants m^{-2}). For each selected plant, the leaves of the main shoot and all primary basal tillers were numbered from one through to the flag leaf to facilitate observations on leaf appearance.

2.3. Observations

To parameterise the leaf area module, data were required on the timing of panicle initiation (PI), the number of tillers per plant, the number of fully expanded and senesced leaves for individual axes and the area of individual leaves. The parameterisation of individual leaf area as a function of total leaf number on an axis has been described in detail in a companion paper (van Oosterom et al., 2001) and will not be considered here.

Timing of PI was determined only for the main shoot through regular dissection of representative plants around the occurrence of PI (Maiti and Bidinger, 1986). Observations were made in the two experiments at Patancheru, plus additional experiments conducted at Patancheru in 1997, some of which included daylength extension treatments.

The number of primary basal tillers and the number of visible, fully expanded, and senesced leaves on each axis were recorded twice a week for all axes of all selected plants, starting directly after thinning (around 10 days after emergence). A leaf was considered visible if its tip extended beyond the ligule of the last fully expanded leaf and was considered fully expanded if the ligule was visible. A leaf was recorded as senesced if >50% of its lamina had senesced. Tillers were numbered according to the main shoot leaf axil from which they appeared. Typically, the first tiller appears from the axil of main shoot Leaf 3 and was labelled T3. A tiller was counted once it had one visible leaf. In order to distinguish productive (panicle bearing) tillers from non-productive ones, a tiller was considered non-productive as soon as the appearance of either new leaf tips or ligules ceased before the flag leaf stage was reached.

In all analyses, time was expressed in degree days, using cardinal temperatures of 10, 33, and 47°C for the base, optimum, and maximum temperature respectively and assuming linear interpolations between these temperatures (Garcia-Huidobro et al., 1982; Ong, 1983a,c; Mohamed et al., 1988).

2.4. Parameterisation of leaf area module

Simulation of GLAI at the individual leaf level in a tillering crop involves the simulation of:

1. The number of leaves for each axis,
2. The rate of appearance of primary basal tillers,
3. The rate of appearance of individual leaves on each axis,
4. The area of individual leaves on each axis,
5. The rate of leaf senescence for each axis.

2.4.1. Estimation of leaf number per axis

The number of leaves on an axis is a function of the leaf initiation rate (LIR) and the duration of the period from germination to PI, which in turn is a function of sowing depth, rate of coleoptile elongation, and photoperiod. Assuming four leaves are already present in the seed, detailed analyses on leaf initiation in pearl millet by Ong (1983a) indicate that leaf initiation starts soon after sowing. Carberry and Campbell (1989) estimated that germination in pearl millet occurs about 5°C d after sowing, whereas linear coleoptile extension starts another 8°C d later. As pearl millet emerges in general 3 days after sowing if sown in a wet soil, we assumed germination to have taken place the day after sowing if sown in a wet soil, or 2 days before emergence if sown in a dry soil and emergence occurred after irrigation. The average photoperiod during the period from emergence to PI was calculated in each experiment by including twilight when the sun is 2.2° below the horizon. As the number of experiments from which we could observe PI was limited to six, our data were complemented by observations (published and unpublished) from experiments carried out at Patancheru between 1978 and 1985 (Alagarswamy and Bidinger, 1985; Carberry and Campbell, 1985; Craufurd and Bidinger, 1988a,b). As all these additional observations had been done on BJ 104, a relationship between time from emergence to PI and daylength was derived for that cultivar only. For the other three cultivars included in our experiments, timing of PI was recorded in six experiments, with a range in photoperiod of about 1.5 h. As this number of observations was too limited to derive any relationship between time to PI and daylength, time to PI in these cultivars was analysed in terms of the difference with BJ 104 in the same experiment.

The LIR was estimated from a regression of total leaf number per axis on thermal time from germination to PI, assuming four leaves were already present in the seed (Ong, 1983a):

$$\frac{1}{\text{LIR}} = \frac{\text{thermal time germination to PI}}{\text{total leaf number} - 4} \quad (1)$$

The data used for deriving the LIR were obtained form experiments conducted during 1996 and 1997 at Patancheru, some of which included daytlength extension treatments.

2.4.2. Estimation of leaf and tiller appearance and death

The rates of leaf appearance (leaf tip and leaf ligule) and of leaf senescence were obtained by plotting leaf numbers as a function of cumulative thermal time after emergence. To avoid confounding effects by non-productive tillers which ceased production of new leaves, only axes that produced a flag leaf were included in this analysis. For each observation date, data were pooled for each cultivar × density× axis combination, making each data point the mean of 6–12 plants. To check the rates of leaf appearance and leaf senescence in non-productive axes (that did not produce a flag leaf), the same procedure was followed for non-productive T3-axes from the rainy season experiment at Patancheru that produced 9 or 10 fully expanded leaves. These axes were used as an example, as they were generally the non-productive tillers that produced most leaves and were thus closest to productive tillers.

The rate of tiller appearance was calculated from the regression of the total number of primary basal tillers on cumulative thermal time after emergence, including only observations taken before the cessation of tiller appearance. For each observation date, data were pooled for each cultivar × density combination, making each data point the mean of 6–12 observations. Once productive tiller number (total minus non-productive) started to decline, the slope of the regression of productive tiller number on thermal time was used to represent the rate at which tillers became non-productive (tillers per °C day).

2.4.3. Leaf size

Methods to estimate the area of individual leaves as a function of total leaf number on an axis have been described by van Oosterom et al. (2001). To use this concept in the estimation of total leaf area, it is imperative to account mathematically for the area of the expanding leaves. Muchow and Carberry (1990) found for sorghum that if x leaves were fully expanded, the total leaf area, including expanding leaves, was best predicted by assuming there were $x + 1.6$ fully expanded leaves. For this concept to work for pearl millet, we needed to establish that leaf expansion rates are similar across axes, and we also needed to verify whether the factor of 1.6 is valid for pearl millet. Because plant density affects the size of the later emerging leaves (van Oosterom et al., 2001), only leaves from plants grown under low densities (4 plants m^{-2}) were used in this analysis.

In order to estimate the adjustment factor for the area of the expanding leaves, we measured the length and width of all expanding leaves of selected axes at a number of occasions in the dry season experiment at Patancheru. The area of these expanding leaves was calculated as length × width × shape factor, using the cultivar-specific shape factors reported by van Oosterom et al. (2001). The cumulative area of the expanding leaves was then compared with their fully expanded area to calculate the leaf number adjustment. The necessary data (number of fully expanded leaves, area of expanding leaves at that moment and when fully expanded), were available for a total of 47 date × cultivar × axis combinations.

The leaf expansion rate was calculated by dividing the leaf length by the duration of leaf expansion. Leaf length was averaged for each combination of cultivar × axis × leaf position within an experiment, irrespective of the total leaf number on the axis. The duration of leaf extension was taken as the duration of the period between the appearance of the leaf tip and of the leaf ligule. The occurrence of both events was estimated from the regression of the number of visible or fully expanded leaves on thermal time from emergence. This is a simplification, because the length of the leaf lamina is already close to 20% of its final leaf length by the time a leaf becomes visible (Lafarge et al., 1998). However, the time between the appearance of the leaf tip and the leaf ligule is roughly equivalent to the duration of linear increase in leaf length (Lafarge et al., 1998) and during this period most of the leaf is elongated (Lafarge et al., 1998). As the absolute leaf elongation rate is constant once a leaf

becomes visible (Tardieu et al., 1999), it can thus be assumed that the errors we introduced were small enough to allow a comparison of expansion rates across axes.

2.5. Dynamics of light competition between axes

In the set-up of APSIM-millet, each axis is considered to be an individual crop. The module currently considers a main shoot and five primary basal tillers. Secondary tillers are not considered, as these seldom become productive. Nodal tillers were not considered either, as these are assumed to be part of the main shoot or basal tiller from which they are produced.

Competition between axes is simulated by using the APSIM-canopy module, which has been specifically designed to deal with intercrops. The main shoot and tillers each have their own defined canopy, and compete for light where canopies are mixed. To calculate the amount of light that is intercepted by each axis, information on the height of each axis is required. The height of a tiller is a linear function of stem weight, assuming 30 cm of height per gram of individual stem weight (including leaf sheath), with a maximum height of 3 m. The vertical distribution of leaf area on an axis is a fifth-power function of the normalised height per axis. This places most of the leaf area per axis at the top of the canopy. From the total LAI per axis and the vertical distribution of LAI, the actual LAI for each axis in canopy layer j can be calculated. The proportion of light entering this layer that is intercepted by that layer (f_j) is a function of the extinction coefficient k_j and the LAI in that layer for axes 1 till n:

$$f_j = 1 - \exp\{-(k_j \mathrm{LAI}_{j1} + \cdots + k_j \mathrm{LAI}_{jn})\} \quad (2)$$

For pearl millet, the extinction coefficient is a function of row spacing, declining from 0.56 at 20 cm row spacing to 0.29 at 150 cm row spacing (van Oosterom et al., unpublished data). The actual amount of light intercepted by axis n in layer j is then calculated using

$$f_{jn} = f_j \left(\frac{k_j \mathrm{LAI}_{jn}}{k_j (\mathrm{LAI}_{j1} + \cdots + \mathrm{LAI}_{jn})} \right) \quad (3)$$

The APSIM-canopy module has been used successfully to simulate growth, development and yield of maize and cowpea in a maize–cowpea intercrop, as well as the biomass of a pasture legume and grain yield of maize in a situation where the legume was sown under the maize, with the two crops competing for light (Carberry et al., 1996).

The pearl millet module was parameterised such that competition for light would kill a tiller if it was unable to set any grains, a situation which would occur if the growth rate at anthesis for an axis was $\leq$0.10 g per day. Once a tiller is killed, it will be left standing in the crop for shading purposes. Its extinction coefficient, however, is reduced to 0.10.

To calculate the effect of competition for resources (light) on the reduction in leaf area, the module first calculates the potential GLAI per axis by using parameter settings for low density conditions; this is especially relevant for the leaf size parameters (van Oosterom et al., 2001). Subsequently, actual GLAI is calculated by incorporating the effect of competition on leaf area expansion through the introduction of maximum bounds on the specific leaf area (SLA) of new leaves. With increasing competition for resources (high plant density), less carbon will be allocated to a particular axis, resulting in thinner leaves (higher SLA) if leaf area is not reduced. Introduction of a maximum bound on SLA will therefore reduce leaf size if competition for light results in limited carbon allocation to an axis.

2.6. Validation of the leaf area module

The leaf area module was validated for the effects of plant density, daylength and cultivar on GLAI (Table 1). Validation was done within APSIM-millet, which was coded as a module of APSIM (McCown et al., 1996). To do the validation runs, the millet module was linked to the soil water module soilwat2, the soil nitrogen module soiln2, and the surface residue module residue2 (Probert et al., 1997). Starting soil conditions were only available for the 1995 validation data sets (Table 1). However, the other experiments were all well-fertilised and were either irrigated or received adequate rainfall (Carberry et al., 1985; Craufurd and Bidinger, 1988a,b, 1989). The effects of drought or nutrient stress on leaf area development in these experiments would therefore have been minimal. Daily minimum and maximum

Table 1
Sowing date, average daylength between emergence and PI, cultivar, plant density, observed and simulated tiller number per plant and reference for data sets from Patancheru that were used for validating the leaf area module and for deriving the maximum specific leaf area. In the simulations, a tiller was considered to be productive if the grain yield exceeded 10 g m^{-2}

Sowing date	Daylength (h)	Cultivar	Plant density (m^{-2})	Productive tiller number (per plant)		Reference
				Observed	Simulated	
Effects of plant density						
19 June 1982	14.0	BJ 104	5.0	4.7	5	Carberry et al. (1985)
19 June 1982	14.0	BJ 104	14.9	1.7	2	Carberry et al. (1985)
19 June 1982	14.0	BJ 104	28.8	1.0	1	Carberry et al. (1985)
Effects of daylength						
19 June 1986	14.0	841A × J 104[a]	12.0	–	2	Craufurd and Bidinger (1989)
19 June 1986	15.5	841A × J 104[a]	12.0	–	1[b]	Craufurd and Bidinger (1989)
Effects of cultivar						
20 June 1995	14.0	WRajPop	6.7	3.0	3[b]	van Oosterom et al. (unpublished)
20 June 1995	14.0	RCB-IC 911	6.7	1.6	2[b]	van Oosterom et al. (unpublished)
Data sets used to derive maximum SLA						
19 June 1982	14.0	BJ 104	40.0	0.7	n/a[c]	Carberry et al. (1985)
21 June 1985	14.0	841A × J 104[a]	9.0	2.9	n/a[c]	Craufurd and Bidinger (1988a,b)
21 June 1985	15.5	841A × J 104a	9.0	2.2	n/a[c]	Craufurd and Bidinger (1988a,b)

[a] Cultivar very similar to BJ 104.
[b] In addition, one tiller which yielded <10 g m^{-2} was simulated.
[c] Not applicable; observed data used as input in the model.

temperature (°C), rainfall (mm) and solar radiation (MJ m^{-2}) were available for each of the validation experiments.

The maximum SLA, used to restrict leaf area in case of reduced carbon allocation to an axis, represents the maximum SLA of new leaves. As this parameter cannot be observed, it had to be derived by manual iteration. Three data sets, for which leaf number and productive tiller number were available, were used for this purpose (Table 1). The maximum SLA was estimated by optimising LAI for these treatments when using observed leaf number as input. None of these treatments were included in the validation data set.

Because actual LAI in the validation runs was determined by carbon restrictions, parameter settings for dry matter accumulation and partitioning were important. Biomass accumulation was simulated using a radiation use efficiency (RUE), based on the interception of total radiation, of 2.17 g MJ^{-1} and an extinction coefficient (based on the interception of total radiation) which declined linearly from a value of 0.56 at a row spacing of 20 cm to a value of 0.29 at a row spacing of 150 cm (van Oosterom et al., unpublished data). For partitioning, 67% of total dry weight was assumed to go to the leaf blade before PI; after PI, this ratio declined linearly until it was zero at the flag leaf stage.

The validation data sets were largely independent of the data sets used for parameterisation. In the parameterisation of the relationship between time to PI and daylength (Fig. 1), the three density data sets (Table 1) together provided one and the two photoperiod data sets (Table 1) provided two data points out of a total of 25. In addition, the two cultivar data sets (Table 1) were part of the analyses used to parameterise the extinction coefficient and the RUE, whereas all validation experiments were used in the parameterisation of biomass allocation (van Oosterom et al., unpublished data). In all these cases, however, the analyses included additional experiments (not used for validation) and parameter estimates were very consistent across experiments. Hence, the independency of the validation data sets from the parameterisation data sets was not significantly compromised.

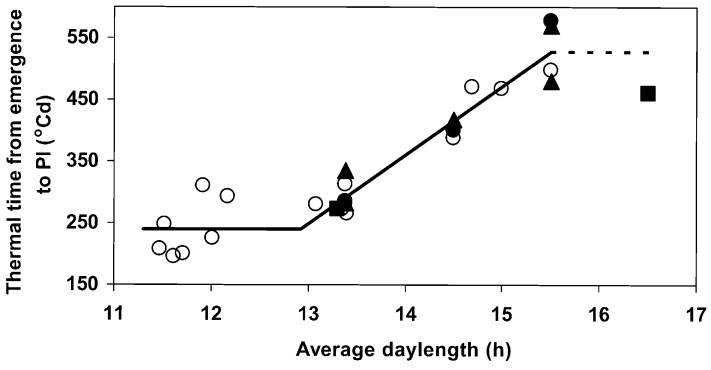

Fig. 1. Thermal time (°C day) from emergence to PI as a function of the average daylength between emergence and PI for pearl millet hybrid BJ 104, grown at Patancheru. Data from this experiment and unpublished data (○), Alagarswamy and Bidinger (1985) (■), Carberry and Campbell (1985) (●) and Craufurd and Bidinger (1988b, 1989) (▲).

3. Results

3.1. Total leaf number

3.1.1. Phenology main shoot

The time from emergence to PI for the main shoot of BJ 104 increased linearly with photoperiod, if photoperiod was above a base photoperiod (Fig. 1). As there were insufficient data to determine the ceiling photoperiod (above which time to PI does not increase anymore), the observations below a daylength of 16 h. were analysed using a piece-wise regression. The fitted regression, was

$$\mathrm{PI} = -1213 + 112.4 \times \mathrm{AVPP} - 112.4 \times (\mathrm{AVPP} - 12.9),$$
$$\text{with} \quad (\mathrm{AVPP} < 12.9), \quad n = 26, \quad R^2 = 0.92 \qquad (4)$$

where AVPP is the average photoperiod between emergence and PI. The base photoperiod, below which time to PI does not decrease further, was 12.9 ± 0.34 h. Under shorter photoperiods, BJ 104 needed about 239°C d from emergence to reach PI. Although the ceiling photoperiod could not be determined accurately, it appeared to be at least 15.5 h, requiring about 530°C d between emergence and PI.

For the six experiments where PI was observed for the other three cultivars, the average time from emergence to PI was 376°C d for BJ 104. The averages for RCB-IC 911 (362°C d) and WRajPop (374°C d) were not significantly different from BJ 104, but the average for HHB 67 (327°C d) was significantly less than BJ 104 ($P < 0.01$, using pairwise comparisons). There was no relationship between the magnitude of this difference and daylength, suggesting that the photoperiod sensitivity of these other cultivars are comparable to BJ 104.

3.1.2. Leaf number on the main shoot and tillers

The number of leaves on the main shoot was a linear function of the time from germination to PI (Fig. 2). Forcing the regression through an intercept of 4 (the number of leaves present at germination) gave an LIR of 0.0368 leaf per °C day ($1/\mathrm{LIR} = 27.2$°C day per leaf):

$$\mathrm{LEAFNR} = 4 + 0.0368 \times \mathrm{PI}, \qquad n = 20, \quad R^2 = 0.80 \qquad (5)$$

As the data included a range of genotypes, the number of observations on individual genotypes was insufficient to detect any cultivar differences in LIR. For tillers, no relationship between leaf number and time to PI could be derived, as data on the timing of tiller initiation were not available. However, leaf number on tillers was estimated relative to the main shoot. On average, T3 had four leaves less than its corresponding main shoot; between T3 and T5, each successive tiller had on average one leaf less than its predecessor, but between T5 and T7, this difference was only about half a leaf (Table 2). These

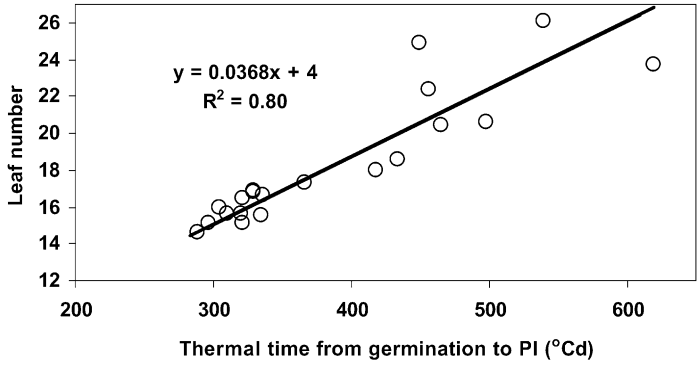

Fig. 2. Relationship between leaf number and time from germination to PI (°C day) for a range of pearl millet cultivars, grown at Patancheru. Data from this experiment and unpublished data collected at Patancheru during 1996 and 1997.

results were not significantly affected by plant density or cultivar.

3.2. Appearance of tillers and leaves

3.2.1. Tiller appearance rate

At Patancheru, tillering generally started in the axil of Leaf 3, but at Jodhpur, for about 15% of plants the first tiller appeared in the axil of Leaf 4 only. This difference between Patancheru and Jodhpur in the fraction of plants producing a T3 was highly significant ($P < 0.001$) according to an χ-test. Occasionally, a tiller appeared in the axil of T2. Tillering started at about 150°C day after emergence in the dry-season experiment at Patancheru (Fig. 3) and at Jodhpur, 1996, but only at 200°C day after emergence in the rainy season experiment at Patancheru.

The number of primary basal tillers was initially a linear function of thermal time. It took successive tillers about 34°C day to appear at Patancheru (Fig. 3), but slightly longer (about 48°C day) at Jodhpur (data not shown). At plant densities >10 plants m^{-2}, tiller appearance ceased around the onset of stem elongation (data not shown). At low densities, however, tiller appearance continued for another 50–100°C day (Fig. 3), resulting in higher tiller numbers at low densities. The effect of cultivar on tillering was relatively small compared with the effects of density (Fig. 3).

3.2.2. Leaf appearance rate

Plant density had no effect on the leaf appearance rate (or its inverse, the phyllochron interval) (Fig. 4), whereas the effect of cultivar was minor, with HHB 67

Table 2
Total leaf number and anthesis date of tillers, expressed as the difference from the total leaf number and anthesis date of the main shoot of the same plant. The number of observations and the standard deviation are also presented. Data obtained from experiments conducted at Patancheru in the dry season and rainy season of 1996 (this paper) and in the rainy season of 1995 and dry season of 1997 (van Oosterom, unpublished).

Axis	Leaf number per axis			Anthesis date		
	Number of observations	Difference main-tiller	Standard deviation	Number of observations	Difference main-tiller (days)	Standard deviation
T2	15	3.07	1.28	13	6.15	3.18
T3	231	3.87	1.07	227	3.11	1.66
T4	241	4.89	1.02	236	3.50	1.98
T5	147	5.95	1.07	143	3.72	1.73
T6	90	6.44	1.17	86	4.83	2.24
T7	45	7.07	1.12	43	5.86	2.18

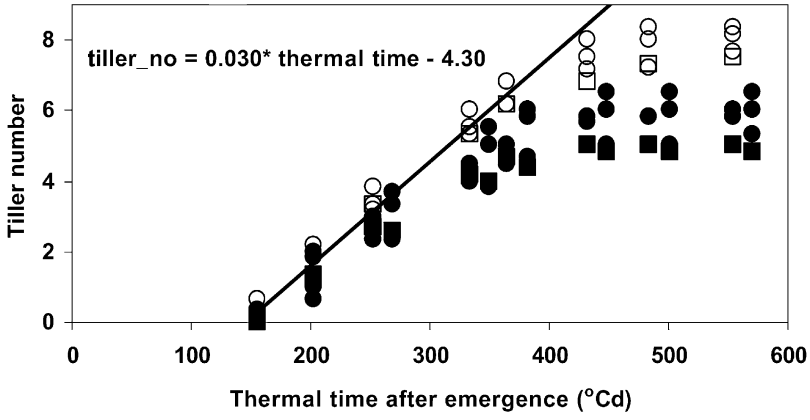

Fig. 3. Number of primary basal tillers at Patancheru in the dry season of 1996 at 4 plants m^{-2} (open symbols) for high-tillering (○) and low-tillering (□) cultivars, and at plant densities >15 plants m^{-2} (closed symbols) for high-tillering (●) and low-tillering (■) cultivars.

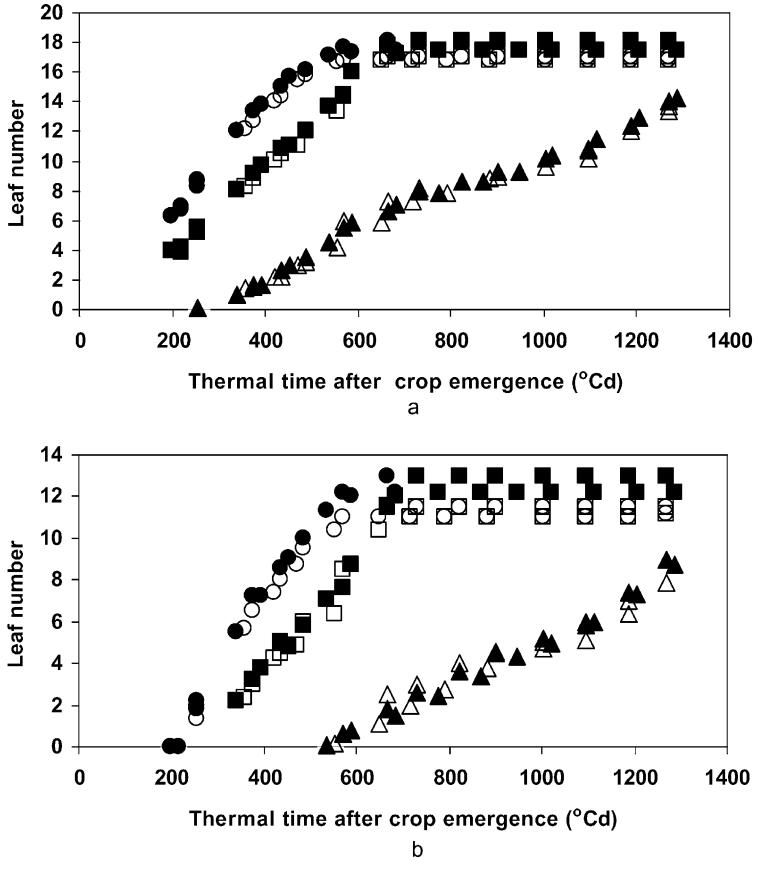

Fig. 4. Number of visible (○, ●), fully expanded (□, ■), and senesced (△, ▲) leaves from crop emergence until physiological maturity for (a) the mainshoot and (b) Tiller 4 of BJ 104 during the rainy season of 1996 at Patancheru, for 4 or 11 plants m^{-2} (closed symbols) and 15 or 20 plants m^{-2} (open symbols). Observations are the mean of 6 or 12 plants.

having a slightly shorter phyllochron interval for fully expanded leaves than the other cultivars. Therefore, for each cultivar × density × axis combination the mean leaf number at each observation date was calculated, using only productive axes, and one single regression analysis of leaf number on thermal time was calculated for each axis, ignoring cultivar× density × axis combinations with only one productive axis.

The number of fully expanded leaves was a linear function of thermal time right until the flag leaf stage (Fig. 4). Leaf appearance rates were similar for the two experiments at Patancheru (Table 3). Across axes, the phyllochron interval, averaged over the two Patancheru experiments, declined from about 35.4°C day per leaf for the main shoot to 42°C day for T6 and T7. Leaves appeared at a slightly slower rate at Jodhpur (Table 3), resulting in longer phyllochron intervals.

The number of visible leaves was a curvilinear function of thermal time and a second order polynomial function adequately fitted the data until the flag leaf stage was reached (Table 3). Leaf tips appeared at a higher rate than leaf ligules for most of the leaf appearance phase, except for the period just before the flag leaf stage, when the rate of ligule appearance slowed down considerably (Fig. 4). For the main shoot, the rate of leaf tip appearance dropped below the appearance rate of the leaf ligule around Leaf 12.5 during the dry season and Leaf 13.1 in the rainy season, which more or less coincided with the position of the largest leaf (van Oosterom et al., 2001).

Differences in leaf number did not significantly affect the appearance rate of leaf ligules (Fig. 4b). There was, however, a small effect on the appearance rate of leaf tips, especially towards the flag leaf stage, when the reduction in leaf tip appearance rates for successive leaves was sharper for tillers with less leaves (Fig. 4b).

Axes that did not produce a fully expanded flag leaf initially tended to develop similarly to productive axes. As an example, Fig. 5 presents data from the rainy season experiment at Patancheru for non-productive T3-axes that produced 9 or 10 fully expanded leaves. The major difference to axes that produced a flag leaf was a distinct drop in the appearance rate of ligules at about 420°C day. This coincided with the cessation of tiller appearance, which in turn was a response to the onset of stem-elongation.

3.2.3. Synchrony in anthesis between axes

Anthesis of the different axes of a plant was highly synchronised, as the later appearance date of successive axes was compensated by a gradual reduction in leaf number. On average, T3 has about four leaves less than the main shoot (Table 2). Using a phyllochron interval of 36.4°C day per leaf (average of main, T3, T4), T3 needs 146°C day less than the main shoot to reach the flag leaf stage. If tiller appearance started 150°C day and successive tillers need 33.9°C day to appear (Fig. 3), T3 appears 184°C day after emergence of the main shoot, and hence reaches anthesis 40°C day later than the main shoot. This difference is close to the observed value of 3.1 days for Patancheru (Table 2). Similarly, each successive tiller has on average one leaf less than its predecessor and hence needs 36°C day less to reach anthesis. Since this difference is comparable to the time successive tillers need to appear (34°C day per tiller), successive tillers reach anthesis at more or less the same time. The observed difference in anthesis date between T3 and T5 was only 0.6 days (Table 2).

3.3. Leaf expansion

As a result of the differences in appearance rates between leaf tips and leaf ligules (Fig. 4, Table 3), the period between the appearance of the tip and the ligule of a leaf increases for successive leaves until the largest leaf is expanding, after which it decreases again. As a result, the longest leaves tended to have the longest duration of leaf expansion. We did not observe any consistent cultivar effect on extension rates and therefore, mean leaf extension rates were calculated across cultivars and the two Patancheru experiments for each ordinal leaf position. In general, extension rates increased with successive leaves until a plateau of about 4.5 mm per °C day was reached at 400–450°C d after emergence (Fig. 6), coinciding with the onset of stem elongation. At Jodhpur, the extension rates of the main shoot followed a similar pattern, but were in general 5% higher than at Patancheru.

The mathematical adjustment factor to account for the area of the expanding leaves was on average 1.45 leaves (Table 4). This means that if there were n fully expanded leaves on an axis, the actual leaf area of that axis was equal to that of a similar axis with $n + 1.45$

Table 3
The number of observations, R^2, the regression of visible leaf number and fully expanded leaf number on thermal time from emergence and the phyllochron interval of fully expanded leaves (per °C day leaf) for individual axes in experiments conducted at Patancheru and Jodhpur in 1996. Each observation represents a cultivar × density × time combination and is the mean of 2–15 observations. Leaf appearance rate is taken as the inverse of the slope of the regression of fully expanded leaf number on thermal time

Axis	Visible leaves			Fully expanded leaves			Phyllochron interval (per °C day leaf)
	Number of observations	R^2	Equation	Number of observations	R^2	Equation	
Patancheru dry season, 1996							
Main	100	0.96	$y = -0.812 + 0.0509\text{TU} - 0.0000359\text{TU}^2$	111	0.98	$y = -0.771 + 0.0280\text{TU}$	35.7
T3	81	0.97	$y = -7.859 + 0.0576\text{TU} - 0.0000381\text{TU}^2$	71	0.96	$y = -5.330 + 0.0273\text{TU}$	36.6
T4	73	0.96	$y = -10.135 + 0.0637\text{TU} - 0.0000439\text{TU}^2$	69	0.95	$y = -5.521 + 0.0254\text{TU}$	39.4
T5	41	0.98	$y = -11.610 + 0.0663\text{TU} - 0.0000464\text{TU}^2$	38	0.95	$y = -6.136 + 0.0254\text{TU}$	39.4
T6	23	0.96	$y = -14.384 + 0.0737\text{TU} - 0.0000523\text{TU}^2$	21	0.94	$y = -6.639 + 0.0247\text{TU}$	40.5
T7	16	0.95	$y = -16.824 + 0.0765\text{TU} - 0.0000534\text{TU}^2$	17	0.96	$y = -7.221 + 0.0232\text{TU}$	43.1
Patancheru rainy season, 1996							
Main	95	0.98	$y = -5.198 + 0.0658\text{TU} - 0.0000478\text{TU}^2$	111	0.97	$y = -2.090 + 0.0285\text{TU}$	35.1
T3	83	0.98	$y = -11.872 + 0.0700\text{TU} - 0.0000493\text{TU}^2$	82	0.96	$y = -6.231 + 0.0269\text{TU}$	37.2
T4	75	0.98	$y = -12.535 + 0.0675\text{TU} - 0.0000463\text{TU}^2$	66	0.94	$y = -7.172 + 0.0266\text{TU}$	37.6
T5	52	0.98	$y = -16.198 + 0.0788\text{TU} - 0.0000584\text{TU}^2$	53	0.90	$y = -7.084 + 0.0239\text{TU}$	41.8
T6	30	0.98	$y = -14.687 + 0.0653\text{TU} - 0.0000422\text{TU}^2$	32	0.93	$y = -7.315 + 0.0222\text{TU}$	45.0
T7	17	0.98	$y = -18.992 + 0.0755\text{TU} - 0.0000489\text{TU}^2$	17	0.96	$y = -9.572 + 0.0252\text{TU}$	39.7
Jodhpur, 1996							
Main				9	1.00	$y = -0.792 + 0.0249\text{TU}$	40.2

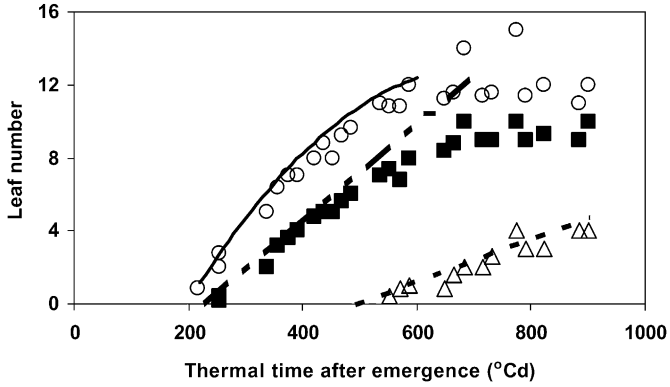

Fig. 5. Number of visible (○), fully expanded (■), and senesced (△) leaves as a function of thermal time (°C day) after emergence for Tiller 3 axes that produced 9 or 10 fully expanded leaves but did not reach flag leaf. Data are from plants grown at Patancheru during the rainy season of 1996 and cover the period until approximately anthesis. Lines represent productive T3 axes, based on the regressions from Table 4 (visible and fully expanded leaves) and Table 5 (senesced leaves).

fully expanded leaves and no expanding leaves. The adjustment factor was very conservative throughout the period of leaf growth, and was also not significantly affected by either axis or cultivar (Table 4).

3.4. Leaf and tiller senescence

3.4.1. Senesced leaf number

Leaf senescence in pearl millet progresses from the bottom of the plant to the top. The rate of leaf senescence was not affected by plant density (Fig. 4). Since genotypic differences were small, a common regression slope across cultivars and densities was calculated for each axis in each experiment (Table 5).

For the main shoot, leaf senescence at Patancheru started at around 180°C day after emergence in the dry season, at around 300°C day after emergence in the rainy season, and 250°C day at Jodhpur (Table 5, Fig. 4a). These differences were partly compensated, however, by a slower rate of leaf senescence before the flag leaf stage in the dry season at Patancheru as compared with the other two experiments. After the flag leaf stage, the rates of leaf senescence declined, although there was a tendency for increased rates

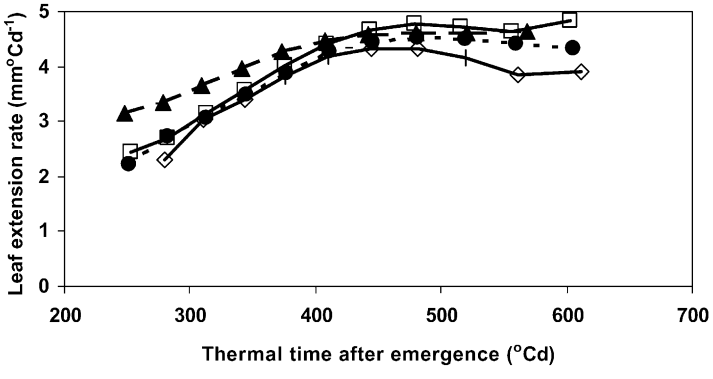

Fig. 6. Leaf extension rates (mm per °C day) as a function of thermal time after emergence for the main shoot (▲–▲), Tiller 3 (□—□), Tiller 4 (●- - -●) and Tiller 5 (◇—◇) at a plant density of 4 plants m^{-2}, averaged over four cultivars and two experiments carried out at Patancheru in 1996. Thermal time was taken as the mean of the appearance of leaf tip and leaf ligule, averaged over the two experiments, using the equations derived in Table 4.

Table 4
The adjustment factor (which accounts for the area of expanding leaves in terms of fully expanded leaf number equivalent), standard deviation, and the number of observations included, expressed as a function of the number of fully expanded leaves, axis, cultivar, and all observations. Data obtained from the dry season experiment, Patancheru, 1996[a]

	Adjustment factor[a]	Standard deviation	Number of observations
Number of fully expanded leaves			
3	1.46 a	0.19	7
4	1.52 a	0.52	9
5	1.27 a	0.27	7
6	1.46 a	0.30	8
7	1.55 a	0.39	7
8	0.84 a	–	1
9	1.65 a	0.17	3
10	1.51 a	0.10	3
11	1.28 a	0.43	2
Axis			
M	1.46 a	0.36	30
T3	1.40 a	0.46	6
T4	1.44 a	0.28	11
Cultivar			
BJ 104	1.44 a	0.30	12
HHB 67	1.51 a	0.30	13
RCB-IC 911	1.42 a	0.45	12
WRajPop	1.43 a	0.32	10
Grand total	1.45	0.35	47

[a] Means followed by the same letter are not significantly different according to a *t*-test for pairwise comparisons.

as physiological maturity was reached (Fig. 4). At physiological maturity, about 3–4 green leaves were still present on each axis. Overall, leaf senescence rates after flag leaf were very similar across experiments (Table 5).

For tillers, leaf senescence started only just before the flag leaf stage was reached (Fig. 4b), which was equivalent to 300°C day after the appearance of that particular tiller (Table 5). As a result, the decline in leaf senescence rate around the flag leaf stage could not be detected in tillers. Senescence rates after the flag leaf stage, however, were similar to those for the main shoots (Table 5). The relatively late onset of leaf senescence in tillers as compared with main shoots (Table 5), combined with their lower leaf numbers (Table 2) but similar leaf senescence rates after the flag leaf stage, resulted in a highly synchronised leaf senescence pattern across tillers. The number of green leaves present on an axis at any time during grain filling was very similar across axes (Fig. 7).

For axes that did not reach the flag leaf stage, leaf senescence progressed for most of the growing season at a rate similar to that of productive tillers (Fig. 5). Tillers that ceased producing new leaves were thus not yet dead, as they still contained green leaves. Such tillers will be referred to as non-productive tillers.

3.4.2. Cessation of tiller growth

Cessation of tiller growth, a sign that tillers would not produce a panicle, started soon after tiller appearance stopped; this was slightly later at low densities (4 plants m^{-2}) than at densities >10 plants m^{-2} (Fig. 8). In general, the first tillers that became non-productive were the ones that were initiated last. The rate at which tillers became non-productive, defined as the absolute value of the slope of the linear part of the decline in tiller number (Fig. 8), increased with increasing plant density, and was higher for RCB-IC 911 than for the other three cultivars (Fig. 8). These effects of density and cultivar on cessation of tiller growth were a result of differences in the GLAI of the main shoot: the rate at which tillers became non-productive was a linear function of the main shoot GLAI at the moment cessation of tiller growth started (Fig. 9).

3.5. Validation of the leaf area module

3.5.1. Parameter settings

The following parameters and equations were used in the validation of the leaf area module:

Estimation of the total leaf number on an axis. The TLN on the main shoot was calculated by combining Eq. (4) (Fig. 1) and Eq. (5) (Fig. 2). For the calculation of daylength, twilight was included when the sun is 2.2° below the horizon. Leaf number on tillers was simulated from the main shoot according to the relationships in Table 2.

Estimation of the timing of appearance of successive tillers. The onset of tillering was set to 150°C day after emergence at Patancheru. Although tillering started slightly later in the rainy season, this delay was probably an artefact, as a similar delay occurred in the appearance of fully expanded leaves (Table 3, intercept of regression line is different). Tiller appearance rate was set to 0.0291 tillers °C per day and the model could simulate a maximum of five primary

Table 5
The number of observations (n), R^2 and the rate of leaf senescence (°C day per leaf), pooled across cultivars and plant densities, for individual axes using all observations and splitting the observations into those before and after full flag leaf appearance. The last column gives the onset of leaf senescence (°C day after emergence of the crop). Each observation is the mean of up to 48 individual observations

Axis	All observations			Before flag leaf appearance[a]			After flag leaf appearance			Onset (°C day)[b]
	n	R^2	Rate (leaf per °C day)	n	R^2	Rate (leaf per °C day)	n	R^2	Rate (leaf per °C day)	
Patancheru dry season, 1996										
M	220	0.98	0.0148	92	0.93	0.0153	128	0.87	0.0123	178
T3	121	0.95	0.0147				99	0.88	0.0131	433
T4	121	0.95	0.0140				99	0.89	0.0133	467
T5	65	0.88	0.0134				62	0.84	0.0133	498
T6	37	0.96	0.0125				36	0.96	0.0126	557
Patancheru rainy season, 1996										
M	200	0.97	0.0132	83	0.94	0.0176	117	0.93	0.0117	297
T3	130	0.95	0.0118				102	0.92	0.0120	496
T4	114	0.93	0.0114				95	0.91	0.0118	560
T5	81	0.93	0.0106				71	0.92	0.0111	617
T6	37	0.87	0.0103				30	0.89	0.0125	686
Jodhpur rainy season, 1996										
M	15	0.98	0.0138	8	0.97	0.0174	7	0.97	0.0113	249

[a] No regression equations for tillers before anthesis, because of the narrow range in thermal time of these observations.
[b] Main shoot: based on observation before full flag leaf emergence only; tillers: based on all observations.

basal tillers. Although more tillers do appear, especially at low plant densities (Fig. 3), the majority of these late tillers cease growing shortly after they appear (Fig. 8) and hence contribute little to total GLAI.

Estimation of the timing of appearance of successive leaves. We used the appearance rate of leaf ligules to determine the phyllochron interval, as this was independent of total leaf number on an axis and was constant throughout the pre-flag leaf stage. A phyllochron interval for leaf ligules of 36.4°C day per leaf was used, representing the mean of the phyllochron intervals of the main shoot, T3, and T4 (Table 3). The error in estimating anthesis date, introduced by using an average leaf appearance rate, would be about 1 day for the main shoot and the first tillers, and up to 3

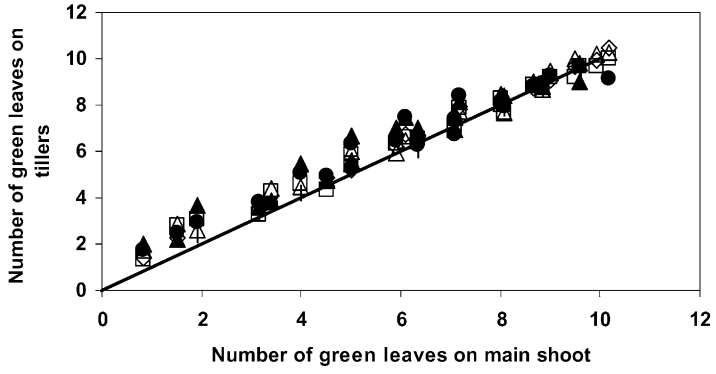

Fig. 7. The number of green leaves on Tiller 3 (△), 4 (◇), 5 (□), 6 (●), and 7 (▲), in relation to the number of green leaves on the main shoot for plants grown at a density of 4 plants m^{-2} at Patancheru during the rainy season of 1996 for three high-tillering cultivars. Each data point is the mean across plants for an individual cultivar at a given date. The solid line is the 1:1 line.

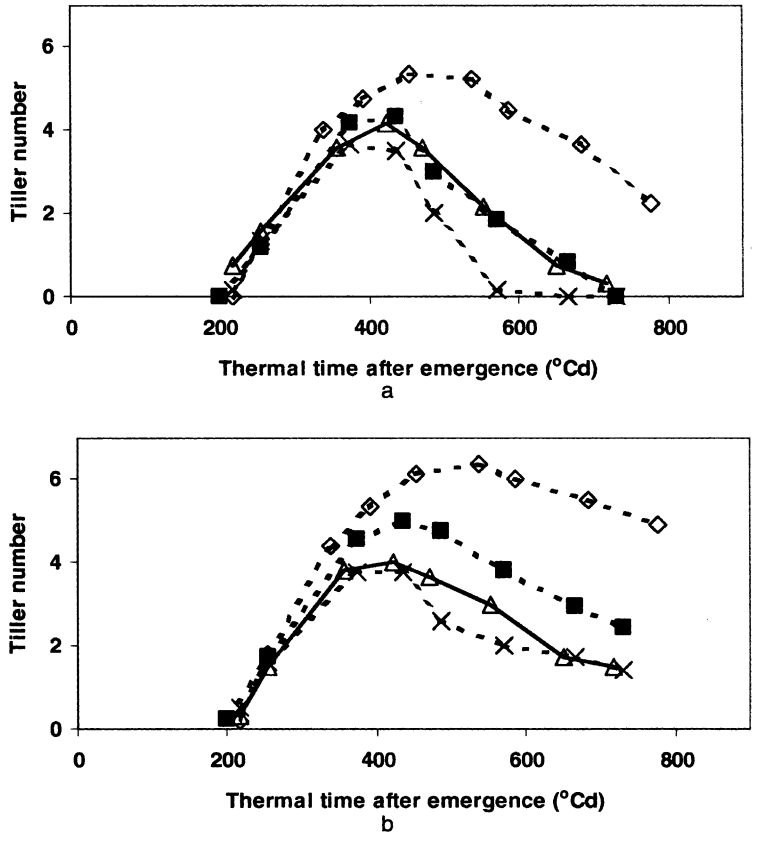

Fig. 8. Number of viable tillers as a function of thermal time after emergence for (a) a low-tillering cultivar and (b) high-tillering cultivars (mean of 3), grown at Patancheru during the rainy season of 1996 at densities of 4 (◇– –◇), 11 (■ – –■), 15 (△—△), and 20 (×– –×) plants m^{-2}.

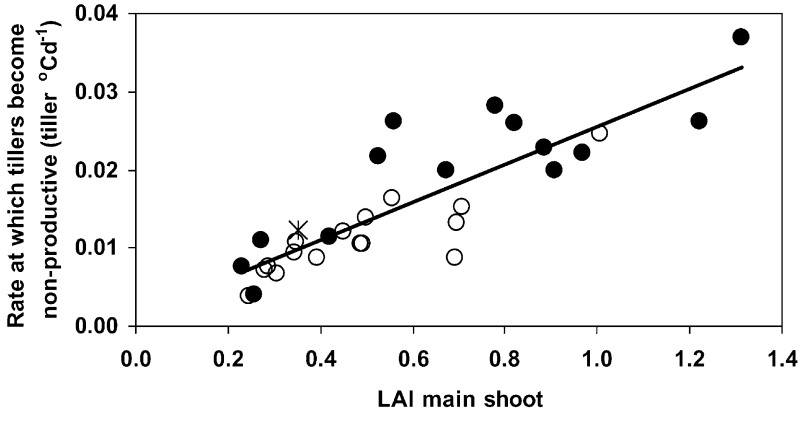

Fig. 9. The rate at which tillers became non-productive during stem elongation, expressed as a function of the GLAI of the main shoot at the onset of tiller death, for four cultivars, grown at Patancheru in the dry season (●) and the rainy season (○) of 1996, and at Jodhpur in 1996 (☆). Fitted regression: rate of cessation = 0.024 LAI + 0.001, $R^2 = 0.74$.

days for the late tillers, assuming a daylength of 13.5 h. In the model, a small adjustment in the appearance rate of the first half leaf was made, to mathematically account for the fact that the regression of fully expanded leaf number on time after emergence did not pass through the origin.

Estimation of mature lamina leaf area of individual leaves. Estimates for X_0, Y_0, a, and b, the parameters that determine the leaf area profile for an axis, were obtained from van Oosterom et al. (2001). For X_0, a, and b, axis-specific parameters were used (cf. Method 5 of van Oosterom et al., 2001). For Y_0, cultivar specific values, derived from experiments conducted at low plant densities (<5 plants m^{-2}), were used, but the effect of axis was restricted to the contrast main shoot versus tillers (van Oosterom et al., 2001).

Estimation of the development of total leaf area per plant. Total leaf area per axis was obtained by summing the area of all fully expanded leaves. The area of the leaves that were still expanding was assumed to equal the area of the next 1.45 leaves after the last fully expanded leaf.

Estimation of the number of senesced leaves on each axis. The onset of leaf senescence was set to 225°C day after emergence for the main shoot and 300°C day after appearance for each tiller. The rate of leaf senescence was set to 0.0167 leaf per °C day until the full appearance of the flag leaf and to 0.0120 leaf per °C day thereafter (Table 5).

3.5.2. Module validation

The first step in validating the leaf area module was to determine an appropriate value for the maximum SLA. To avoid confounding effects of errors in simulated leaf numbers on the simulation of LAI, observed main shoot leaf numbers were used as input in the model. In addition, leaf numbers for productive tillers were estimated from Table 2, whereas for non-productive tillers, leaf numbers were estimated from relationships between main shoot leaf number and

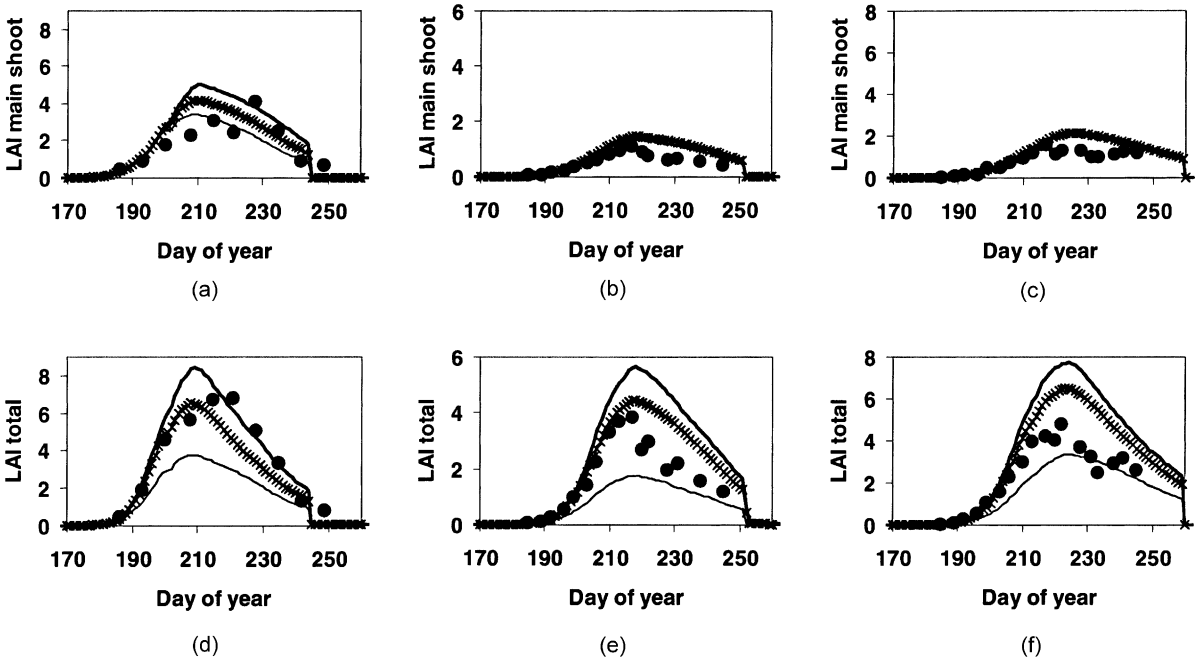

Fig. 10. Observed (●) and simulated GLAI for the main shoot (a–c), and total crop (d–f), for plants grown at Patancheru during the rainy season of 1982 under normal daylength at 40 m^{-2} plants (a,d), and during the rainy season of 1985 at 9 plants m^{-2} under normal (b,e) and extended (c,f) daylength, using different values for the maximum specific leaf area (SLA_MAX): thin line, SLA_MAX = 300 $cm^2\ g^{-1}$; thick line, SLA_MAX = 999 $cm^2\ g^{-1}$ and ×××-line, SLA_MAX declines linearly from 650 $cm^2\ g^{-1}$ at LA ≤ 2 to 450 $cm^2\ g^{-1}$ at LAI ≥5. Observed data from Carberry and Campbell (1985) and Craufurd and Bidinger (1988a,b).

leaf number on non-productive tillers, based on observations from the 1996 experiments.

If there were no carbon restrictions on leaf expansion (maximum SLA = 999 $cm^2\ g^{-1}$), GLAI was over-estimated (Fig. 10). This over-estimation occurred mainly in the tillers, except for the high density in 1982. The likely reason for this was that under this extremely high plant density, only one tiller was producing a significant amount of leaves, with the remaining tillers producing <5 leaves. The overestimation of LAI in tillers at the lower plant densities indicated that tiller leaves were allowed to grow too thinly (maximum SLA too high) if carbon supply was limited. A limit of 300 $cm^2\ g^{-1}$, by contrast, underestimated GLAI, especially in the tillers (Fig. 10). There was little effect on the LAI of the main shoot at a density of 9 plants m^{-2} (Fig. 10b and c), but a significant effect at the high plant density (Fig. 10a). The underestimation of tiller-LAI indicates that if sufficient carbon is available, leaves were not able to grow to their full potential (maximum SLA too low). On average, the best results were obtained if maximum SLA was set to a value of about 650 $cm^2\ g^{-1}$ (Fig. 10). As maximum SLA is expected to decline as LAI increases, it was set to a value of 650 $cm^2\ g^{-1}$ if GLAI <2, dropping linearly to a value of 450 $cm^2\ g^{-1}$ between GLAI = 2 and GLAI = 5, with GLAI representing the LAI of individual axes.

The millet module in general accurately captured the effects of plant density (Fig. 11), photoperiod (Fig. 12), and cultivar (Fig. 13) on GLAI. In the density data set (Fig. 11), the module slightly under-estimated the GLAI of tillers during grain filling, but it reproduced the observation that the GLAI of tillers did not increase much beyond a plant density of 15 plants m^{-2}. The effect of plant density on productive tiller number was also reproduced by the module (Table 1). The module simulated the increase in GLAI under extended daylength (Fig. 12) correctly, both for main shoots and tillers, despite the slight over-estimation

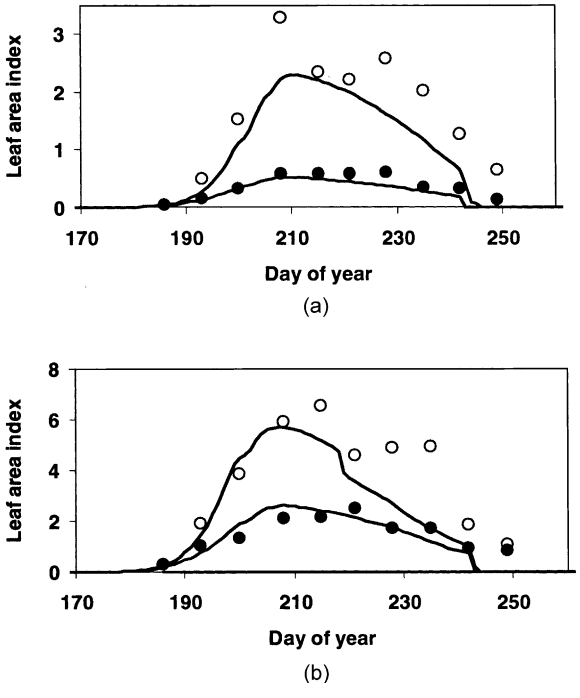

Fig. 11. Observed GLAI for the main shoot (●) and the total crop (○) and simulated GLAI (—) for plants grown at Patancheru during the rainy season of 1982 at plant densities of (a) 5 plants m^{-2} and (b) 29 plants m^{-2}. Observed data from Carberry et al. (1985).

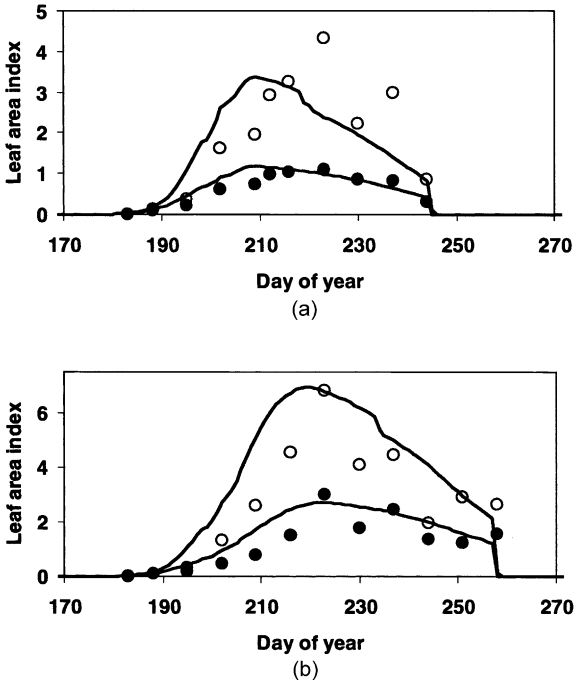

Fig. 12. Observed GLAI for the main shoot (●) and the total crop (○) and simulated GLAI (—) for plants grown at Patancheru during the rainy season of 1986 under (a) normal and (b) extended daylength. Observed data from Craufurd and Bidinger (1989).

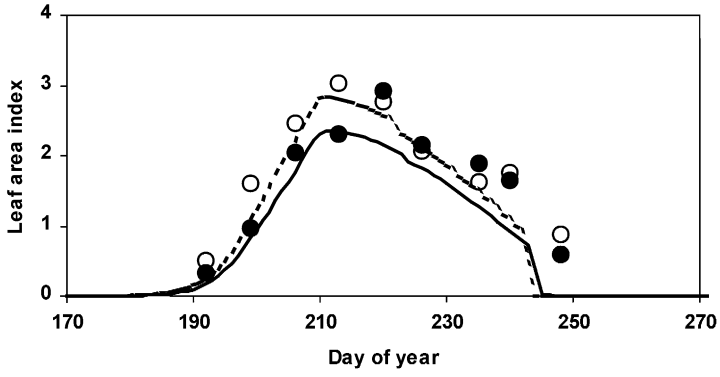

Fig. 13. Observed and simulated (—) GLAI for the total crop of WRajPop (●) and RCB-IC 911 (○), grown in the rainy season of 1995 at Patancheru, at a density of 6.7 plants m^{-2}.

of GLAI early in the season. Although no data were available on observed productive tiller number, the reduction in simulated tiller number under longer daylength was in accordance with observations by Craufurd and Bidinger (1988b) for the same genotype. The module also reproduced the genotypic differences in LAI and productive tiller number, resulting from differences in leaf size (Fig. 13, Table 1). Importantly, the model provided a realistic distribution of leaf area across individual tillers, reproducing the lower GLAI for tillers which were initiated later (Fig. 14).

4. Discussion

This paper and the previous one (van Oosterom et al., 2001) describe the parameterisation and validation of a module to simulate GLAI in pearl millet. The module is based on the simulation of the green leaf area of individual leaves on an axis, and involves the simulation of (1) the final leaf number per axis as a function of photoperiod and thermal time (Figs. 1 and 2, Table 2), (2) the appearance of individual axes as a function of thermal time (Fig. 3), (3) the appearance of fully expanded leaves on individual axes as a function of thermal time (Table 3), (4) the area of individual leaves on an axis as a function of total leaf number (van Oosterom et al., 2001), and (5) the number of dead leaves on an axis as a function of thermal time (Table 5). This approach has been used successfully to simulate GLAI in non-tillering sorghum (Carberry and Abrecht, 1991), maize (Keating and Wafula, 1992), and tillering sorghum (Carberry et al., 1993b). We have incorporated the individual leaf area approach into a module that dynamically simulates GLAI through accounting for the effects of competition for light between tillers, in order to deal with genotypic and environmental variation in productive tiller number. This intercrop approach to simulate tillering is a novel concept in the simulation of GLAI, and is particularly useful given large genotypic variation in leaf size in pearl millet.

4.1. Parameterisation of the leaf area module

4.1.1. Phenology

Phenology is important for the GLAI module, as time to PI and LIR together determine the final leaf number on an axis and hence GLAI. In our analyses, the minimum thermal time from emergence to PI was about 239°C day, whereas the maximum was about 530°C day. A recalculation of data from a greenhouse experiment by Ong and Everard (1979), who used cultivars similar to ours, yielded values of about 280–300°C day under short daylength (12 h) and 560–590°C day under long daylength (17.2 h), based on their average soil temperature of 24°C and assuming 3 days from sowing to emergence. The similarity in maximum duration confirms that our estimate of 15.5 h for the ceiling photoperiod is relatively accurate. A more precise estimate is not required, as pearl millet is generally grown from tropical to subtropical latitudes where daylength does not exceed 15.5 h. The time needed for successive leaves to initiate

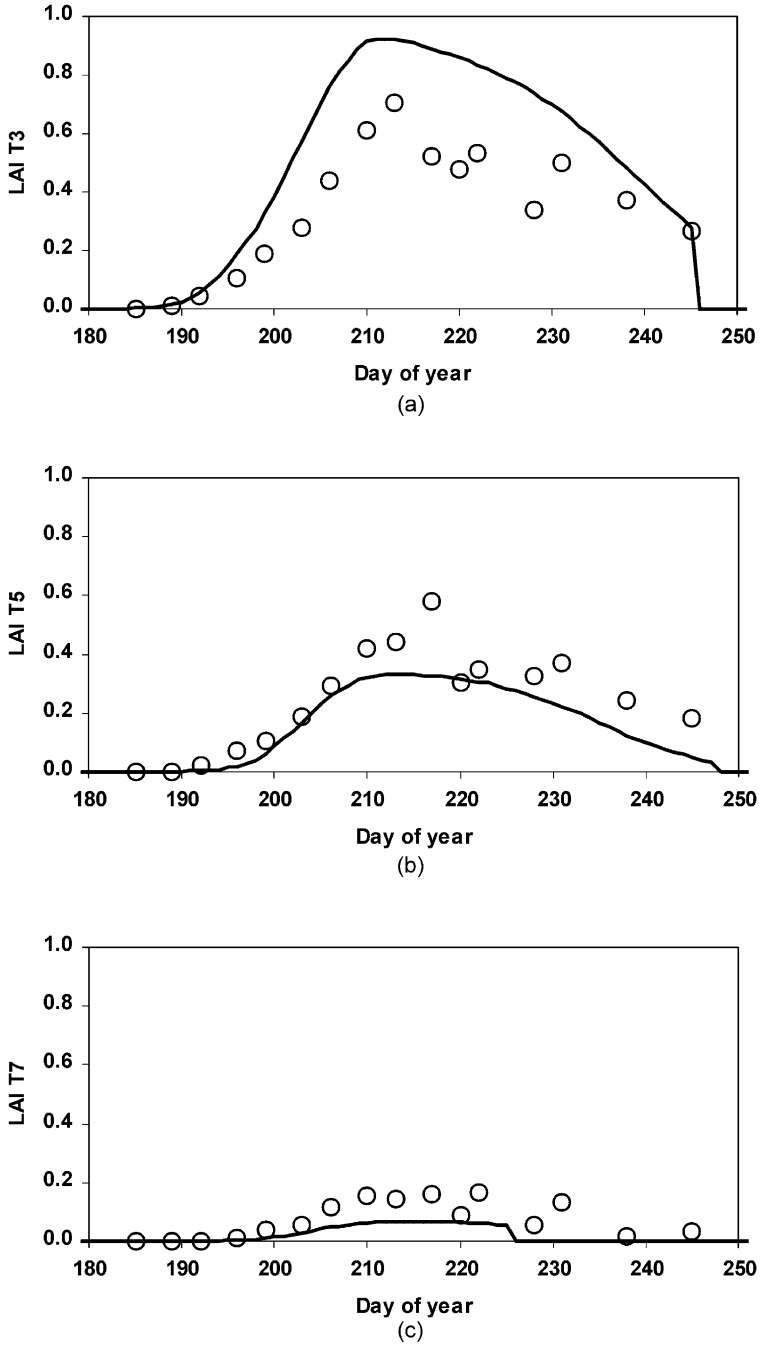

Fig. 14. Observed (○) and simulated (—) GLAI for (a) T3, (b) T5, and (c) T7 for plants grown at Patancheru during the rainy season of 1985 under normal daylength at a density of 9 plants m^{-2}. Observed data from Craufurd and Bidinger (1988a,b).

(27.2°C day per leaf, Eq. (5)) compares well with the value of 25.6°C day per leaf observed by Ong (1983a). The slightly lower value of Ong (1983a) can be attributed to the use of a slightly higher T_{base} (11.3°C). In the phenology module we used, the timing of the flag leaf stage is a function of the product of leaf appearance rate and leaf number. Hence, the duration of the stage between PI and flag leaf is a consequence of the difference between the estimated occurrence of PI and anthesis, and is not itself an input into the model. However, because the LIR is only marginally faster than the leaf appearance rate, an increase in leaf number will delay PI to nearly the same extent as anthesis. As a result, the period between PI and anthesis is relatively constant, confirming observations by Craufurd and Bidinger (1988a), although it is a function of the number of leaves produced prior to PI (Coaldrake and Perason, 1985).

Leaf numbers on tillers were estimated from those on main shoots (Table 2). Hence, GLAI of tillers was not determined by the phenology of the tillers, but rather by the phenology of the main shoot. The reason was the limited availability of data on the timing of PI in tillers. In addition, tillers have been growing substantially before they emerge from the sheath of the subtending leaf (Lafarge et al., 1998), and it is thus likely several leaves have already been initiated in a tiller by the time it appears. In order to estimate leaf number in a tiller from the LIR, it is therefore necessary to estimate the onset of leaf initiation in the tiller. Tillers are derived from auxiliary buds, which are likely to be similar to the embryo. In that case, four leaves will be initiated in the bud. As T3 has on average four leaves less than the main shoot, the duration of the leaf initiation period will be about 100°C day less for T3 than the main shoot, assuming that the LIR is the same across axes. Craufurd and Bidinger (1988a) observed that PI in T3 occurred about 30°C day later than in the main shoot, irrespective of daylength. This means that leaf initiation in T3 would have started approximately 130°C day after germination (approximately 100°C day after emergence), irrespective of daylength. This difference with the onset of tillering (150°C day) can be accounted for by the time it takes for the tip of the first leaf of a tiller to elongate above the ligule of the subtending main shoot leaf. Similarly, for each successive tiller, PI occurred about 15–20°C day later than for its predecessor (Craufurd and Bidinger, 1988a). As each tiller has about one leaf less than its predecessor (Table 2) and hence needs 25°C day less to reach PI, each successive tiller will start initiation of leaves about 40–45°C day later than its predecessor. This period is comparable to the 43°C day that elapsed between the appearance of two successive tillers as observed in the same experiment (Craufurd and Bidinger, 1988a). Although the above mechanism for the onset of leaf initiation in tillers is speculative, it provides a direct link between the start of leaf initiation in tillers and their appearance. However, more data on the onset of leaf initiation in tiller buds are required before these data can be used in future versions of APSIM-millet.

4.1.2. Appearance and senescence of leaves and tillers

Tillering started in our experiment at around 150°C day after emergence, which is comparable to the values of 140–185°C day observed by Ong (1983a) and Craufurd and Bidinger (1988a). The period of 34.4°C day, required for the appearance of successive tillers at Patancheru, was slightly shorter than the 43°C day per tiller reported by Ong (1984) and Craufurd and Bidinger (1988a). The discrepancy could be attributed to the fact that we used the maximum tiller appearance rates; using the average tiller appearance rate of the high-tillering cultivars at densities >13 plants m^{-2} (Fig. 3) also yielded a value of about 43°C day per tiller.

The appearance rate of leaf ligules was independent of the total leaf number on an axis. In addition, leaf extension rates were relatively constant. The maximum leaf extension rates of approximately 4.0–4.5 mm per °C day in our experiments (Fig. 6) compared well with the value of 4 mm per °C day obtained by Ong (1983b) using auxonometers. Because leaf size tends to increase with leaf number (van Oosterom et al., 2001), the duration of the extension of individual leaves increases with increasing leaf number. This was accommodated through changes in the appearance rate of leaf tips, rather than leaf ligules, confirming results of Triboi and Ntonga (1993). Therefore, simulation of leaf appearance is preferably done using leaf ligules.

The phyllochron interval for the main shoot (35–36°C day per leaf; Table 3) was comparable to

the 33–34°C day per leaf observed by Craufurd and Bidinger (1988a). However, Ong (1983a, 1984) observed slightly faster rates of 24–25°C day per leaf, based on a T_{base} of 12–13°C; this translates to about 30°C day per leaf using a T_{base} of 10°C. Although the phyllochron interval increased slightly for later tillers, differences between axes were relatively small, confirming observations for both sorghum (Carberry et al., 1993b) and pearl millet (Craufurd and Bidinger, 1988a; Ong, 1984). The factor for the area of the expanding leaves which we observed (1.45) is close to the value of 1.6 identified for sorghum by Muchow and Carberry (1990).

Leaf senescence could be divided into two stages: a high rate of leaf senescence before the flag leaf stage, and a lower rate thereafter. The high turn-over rate of leaves before the flag leaf stage was mainly due to the senescence of leaves that were produced before PI. These leaves remained close to the ground level after the onset of stem elongation, and hence could not capture sufficient light once stem elongation started. Our results confirm comparable observations for sorghum (Carberry et al., 1993a; Borrell et al., 2000). Borrell et al. (2000) even identified a third stage of rapid leaf senescence towards the end of grain filling. Although there were signs in our experiments of an accelerated leaf senescence towards physiological maturity (Fig. 4), this phenomenon is particularly important under conditions of stress, but is relatively insignificant under optimum conditions. Carberry et al. (1993a) described the rate of leaf senescence using relative leaf number, rather than absolute leaf number. In our study, leaf senescence was best expressed using absolute leaf number. This was confirmed by observations on four pearl millet varieties from West Africa, which had leaf senescence rates very similar to BJ 104, despite substantial differences in phenology (van Oosterom, unpublished data).

4.2. Validation of the leaf area module

The leaf area module generally simulated GLAI well. The good agreement between observed and simulated GLAI during leaf area expansion and leaf senescence indicates that the relevant parameter estimates were appropriate, confirming the agreement between our observations and other published data. This indicates that the concept of simulating GLAI from total leaf number on an axis and individual leaf size is useful, despite the conclusion by Elings (2000) that the predictive application of the parameters that define individual leaf size is restricted. That conclusion, however, was based on an analysis of leaf area profiles that included drought and N-stressed environments. Such an analysis ignores the fact that stress will alter the shape of the leaf area profile curve (van Oosterom et al., 2001). In fact, preliminary simulations of an experiment including three N-treatments indicated that APSIM-millet is capable of reproducing the effects of N-deficiency on LAI (van Oosterom, unpublished data). The good simulation of LAI was also in spite of a weak relationship between the area of the largest leaf (Y_0) and total leaf number on an axis (van Oosterom et al., 2001). This poor relationship, however, merely reflects the heterogeneous nature of some of the open-pollinated varieties and landraces used in our experiments. As our relationships between Y_0 and total leaf number are based on many observations (van Oosterom et al., 2001), it can be assumed that they adequately represent the mean Y_0 for a given leaf number. The good simulation results thus show that heterogeneity of pearl millet within the crop does not necessarily have a negative effect on the capability to simulate crop GLAI.

The millet module simulates a maximum of five tillers. Although more tillers are produced throughout the life cycle of the crop, especially if secondary tillers are considered, most of these tillers become non-productive, even at low plant densities (Fig. 8; Craufurd and Bidinger, 1988a). Their contribution to total GLAI is expected to be relatively small and that to biomass even smaller, as these non-productive tillers do not elongate. They will hence contribute little to photosynthesis, as their leaves are located at the bottom of the canopy. The number of tillers that can be simulated by APSIM-millet can be increased, but the errors introduced by simulating a maximum of five tillers are expected to be minor in most circumstances.

The observed effects of density, photoperiod, and genotype on tillering were reproduced adequately by the module, although the mechanism used to achieve these results was over simplified. In general, non-productive tillers cease producing new leaves when the main stem is elongating (Fig. 5; Craufurd and Bidinger, 1988a). This is most likely due to shading of

the later-initialised tillers and to changing patterns of assimilate redistribution within the plant at stem elongation. However, tillers which cease producing new leaves will not die until leaf senescence has caught up with the number of green leaves that has been produced (Fig. 5). The size of the leaves that appear on these non-productive axes, however, is in general not much smaller than that of comparable leaves on productive axes (van Oosterom, unpublished data). The reduction in leaf area of non-productive tillers is thus a result of a reduction in leaf number, rather than in individual leaf size. In our validation runs, however, tillers only died at anthesis as a result of barrenness, and hence all reached flag leaf. Consequently, the reduced leaf area per tiller in the simulation runs is a result of a reduction in leaf size. This mechanism is evident in the runs for individual tillers (Fig. 14), where leaf area of T5 and T7 was negligible and close to observed, although the model simulated 10.3 and 9.3 leaves per axis, respectively. Although the mechanism employed in APSIM-millet to reduce leaf area under light competition is a simplification, the simulated seasonal pattern of LAI and the simulated productive tiller number were close enough to observed values to justify the current routines for tiller death in the module.

The current set up of the module, where each axis is considered to be a crop, offers flexibility in simulating cultivar differences in GLAI without increasing the need for parameterisation. Although each axis is parameterised separately, most of the parameters derived in this paper and the previous one (van Oosterom et al., 2001) appear to be conservative across axes. The main exceptions are those which relate to the leaf area profile. However, as these parameters are conservative across cultivars (at least in our experiments), the values used in the current module should be applicable across a wide range of cultivars. The only parameters which are dependent on both cultivar and axis are those that describe the relationship between the size of the largest leaf on an axis and the total leaf number on that axis. These are important parameters, as they affect GLAI of the main shoot and hence tiller survival (Fig. 9). The dynamic set up of the module, however, also reduces over-parameterisation that would be required by a more empirical approach. An important example of this in APSIM-millet is the simulation of tillering, where our results show that differences in tillering can be simulated without an explicit cultivar-specific tillering parameter. However, cultivar differences in tillering that are not associated with differences in main shoot GLAI can be captured by changing the growth rate (at anthesis) below which a tiller does not produce any grain anymore. In theory, such flexibility should enable APSIM-millet to simulate cultivar $\times$ environment interactions for GLAI and tiller survival.

5. Conclusions

This paper and the previous one (van Oosterom et al., 2001) present data on the development and validation of a module for estimating GLAI for pearl millet. It is based on the competition for resources between the main shoot and each individual tiller. Potential GLAI is calculated for each axis, based on the area of individual leaves, and actual GLAI is then calculated by incorporating the effects of resource allocation between axes. The module adequately simulated seasonal patterns for total crop GLAI for experiments covering differences in plant density, photoperiod, and cultivar, and provided a realistic partitioning of total GLAI between main shoots and tillers.

Acknowledgements

We would like to acknowledge the excellent assistance of D. Dharani, M. Kistaiah and M.M. Sharma in managing the field experiments and collecting the data. Dr. N.L. Joshi of the Central Arid Zone Research Institute, Jodhpur, India, is acknowledged for facilitating the experiments conducted at that site. Dr. P.Q. Craufurd is acknowledged for providing us with the original of his published data to allow validation of the GLAI module. Drs. G.L. Hammer and M.J. Robertson are thanked for their useful comments on earlier versions of the manuscript. This work was part of the CARMASAT project, jointly funded by the Australian Centre for International Agricultural Research (ACIAR) and ICRISAT. Drs. R.J.K. Myers and R.L. McCown, CARMASAT co-leaders, and M.M. Anders, project leader at ICRISAT, are thanked for their support in conducting the research.

References

Alagarswamy, G.A., Bidinger, F.R., 1985. The influence of extended vegetative development and d_2 dwarfing gene in increasing grain number per panicle and grain yield in pearl millet. Field Crops Res. 11, 265–279.

Asseng, S., Keating, B.A., Fillery, I.R.P., Gregory, P.J., Bowden, J.W., Turner, N.C., Palta, J.A., Abrecht, D.G., 1998. Performance of the APSIM-wheat model in Western Australia. Field Crops Res. 57, 163–179.

Bidinger, F.R., Raju, D.S., 2000. Mechanisms of adjustment by different pearl millet plant types to varying plant populations. J. Agric. Sci. Camb. 134, 181–189.

Borrell, A.K., Hammer, G.L., Douglas, A.C.L., 2000. Does maintaining green leaf area in sorghum improve yield under drought? 1. Leaf growth and senescence. Crop Sci. 40, 1026–1037.

Carberry, P.S., Abrecht, D.G., 1991. Tailoring crop models to the semiarid tropics. In: Muchow, R.C., Bellamy, J.A. (Eds.), Climatic Risk in Crop Production: Models and Management for the Semiarid Tropics and Subtropics. CAB International, Wallingford, pp. 157–182.

Carberry, P.S., Campbell, L.C., 1985. The growth and development of pearl millet as affected by photoperiod. Field Crops Res. 11, 207–217.

Carberry, P.S., Campbell, L.C., 1989. Temperature parameters useful for modelling the germination and emergence of pearl millet. Crop Sci. 29, 220–223.

Carberry, P.S., Campbell, L.C., Bidinger, F.R., 1985. The growth and development of pearl millet as affected by plant population. Field Crops Res. 11, 193–205.

Carberry, P.S., Hammer, G.L., Muchow, R.C., 1993a. Modelling genotypic and environmental control of leaf area dynamics in grain sorghum. III. Senescence and prediction of green leaf area. Field Crops Res. 33, 329–351.

Carberry, P.S., Muchow, R.C., Hammer, G.L., 1993b. Modelling genotypic and environmental control of leaf area dynamics in grain sorghum. II. Individual leaf level. Field Crops Res. 33, 311–328.

Carberry, P.S., Adiku, S.G.K., McCown, R.L., Keating, B.A., 1996. Application of the APSIM cropping systems model to intercropping systems. In: Ito, O., Johansen, C., Adu-Gyamfi, J.J., Katayama, K., Kumar Rao, J.V.D.K., Rego, T.J. (Eds.), Dynamics of Roots and Nitrogen in Cropping Systems of the Semi-arid Tropics. Proceedings of the International Workshop, held at the International Crops Research Institute for the Semi-Arid Tropics (ICRISAT), Patancheru 502 324, Andhra Pradesh, India, November 21–25, 1994. Japan International Research Center for Agricultural Sciences (JIRCAS) International Agriculture Series No. 3. JIRCAS, Japan, pp. 637–648.

Coaldrake, P.D., Perason, C.J., 1985. Development and dry weight accumulation of pearl millet as affected by nitrogen supply. Field Crops Res. 11, 171–184.

Craufurd, P.Q., Bidinger, F.R., 1988a. Effect of duration of the vegetative phase on shoot growth, development and yield in pearl millet (*Pennisetum americanum* (L.) Leeke). J. Exp. Bot. 39, 124–139.

Craufurd, P.Q., Bidinger, F.R., 1988b. Effect of the duration of the vegetative phase on crop growth, development and yield in two contrasting pearl millet hybrids. J. Agric. Sci. Camb. 110, 71–79.

Craufurd, P.Q., Bidinger, F.R., 1989. Potential and realized yield in pearl millet (*Pennisetum americanum*) as influenced by plant density and life cycle duration. Field Crops Res. 22, 211–225.

Elings, A., 2000. Estimation of leaf area in tropical maize. Agron. J. 92, 436–444.

Frère, M., Popov, G.F., 1979. Agrometeorological crop monitoring and forecasting. FAO Plant Production and Protection Paper No. 17. FAO, Rome, Italy.

Garcia-Huidobro, J., Monteith, J.L., Squire, G.R., 1982. Time, temperature and germination of pearl millet (*Pennisetum typhoides* S. and H.). J. Exp. Bot. 33, 288–296.

Huda, A.K.S., Sivakumar, M.V.K., Alagarswamy, G., Virmani, S.M., Vanderlip, R.L., 1984. Problems and prospects in modelling pearl millet growth and development: a suggested framework for a millet model. In: Virmani, S.M., Sivakumar, M.V.K. (Eds.), Agrometeorology of Sorghum and Millet in the Semi-arid Tropics, Proceedings of the International Symposium, November 15–20, 1982, International Crops Research Institute for the Semi-Arid Tropics (ICRISAT), India. ICRISAT, Patancheru 502 324, AP, India.

Keating, B.A., Wafula, B.M., 1992. Modelling the fully expanded area of maize leaves. Field Crops Res. 29, 163–179.

Lafarge, T., de Raïssac, M., Tardieu, F., 1998. Elongation rate of sorghum leaves has a common response to meristem temperature in diverse African and European environmental conditions. Field Crops Res. 58, 69–79.

Maiti, R.K., Bidinger, F.R., 1986. Growth and development of the pearl millet plant. Research Bulletin No. 6, International Crops Research Institute for the Semi-Arid Tropics (ICRISAT), Patancheru, India, 14 pp.

McCown, R.L., Hammer, G.L., Hargreaves, J.N.G., Holzworth, D.P., Freebairn, D.M., 1996. APSIM: a novel software system for model development, model testing and simulation in agricultural systems research. Agric. Syst. 50, 255–271.

Meinke, H., Hammer, G.L., van Keulen, H., Rabbinge, R., 1998. Improving wheat simulation capabilities in Australia from a cropping systems perspective. III. The integrated wheat model (I-WHEAT). Eur. J. Agron. 8, 101–116.

Mohamed, H.A., Clark, J.A., Ong, C.K., 1988. Genotypic differences in the temperature responses of tropical crops. III. Light interception and dry matter production of pearl millet (*Pennisetum typhoides* S.H.). J. Exp. Bot. 39, 1137–1143.

Muchow, R.C., Carberry, P.S., 1990. Phenology and leaf area development in a tropical grain sorghum. Field Crops Res. 23, 221–237.

O'Leary, G.J., Connor, D.J., 1996. A simulation model of the wheat crop in response to water and nitrogen supply. I. Model construction. Agric. Syst. 52, 1–29.

Ong, C.K., 1983a. Response to temperature in a stand of pearl millet (*Pennisetum typhoides* S. and H.). 1. Vegetative development. J. Exp. Bot. 34, 322–336.

Ong, C.K., 1983b. Response to temperature in a stand of pearl millet (*Pennisetum typhoides* S. and H.). 2. Reproductive development. J. Exp. Bot. 34, 337–348.

Ong, C.K., 1983c. Response to temperature in a stand of pearl millet (*Pennisetum typhoides* S. and H.). 4. Extension of individual leaves. J. Exp. Bot. 34, 1731–1739.

Ong, C.K., 1984. Response to temperature in a stand of pearl millet (*Pennisetum typhoides* S. and H.). v. Development and fate of tillers. J. Exp. Bot. 35, 83–90.

Ong, C.K., Everard, A., 1979. Short day induction of flowering in pearl millet (*Pennisteum typhoides*) and its effect on plant morphology. Expl. Agric. 15, 401–410.

Probert, M.E., Dimes, J.P., Keating, B.A., Dalal, R.C., Strong, W.M., 1997. APSIM's water and nitrogen modules and simulation of the dynamics of water and nitrogen in fallow systems. Agric. Syst. 56, 1–28.

Tardieu, F., Granier, C., Muller, B., 1999. Modelling leaf expansion in a fluctuating environment: are changes in specific leaf area a consequence of changes in expansion rates? New Phytol. 143, 33–43.

Triboi, E., Ntonga, J., 1993. Effect of nitrogen and light intensity on the development of leaves and spikes of winter wheat (Effet de l'azote et du rayonnement sur le developpement des feuilles et de l'epi chez le ble d'hiver: mise en place de l'appareil foliaire et de la structure de l'epi). Agronomie 13, 253–265.

van Evert, F.K., Campbell, G.S., 1994. CropSyst: a collection of object oriented simulation models of agricultural systems. Agron. J. 86, 325–331.

van Keulen, H., Seligman, N.G., 1987. Simulation of Water Use, Nitrogen Nutrition and Growth of a Spring Wheat Crop. Pudoc, Wageningen, The Netherlands, 310 pp.

van Oosterom, E.J., Acevedo, E., 1992. Adaptation of barley (*Hordeum vulgare* L.) to harsh Mediterranean environments. II. Apical development, leaf, and tiller appearance. Euphytica 62, 15–27.

van Oosterom, E.J., Carberry, P.S., O'Leary, G.J., 2001. Simulating growth, development, and yield of tillering pearl millet. 1. Leaf area profiles on main shoots and tillers. Field Crops Res. 72, 51–66.